

Supporting Information

Rapid, All Dry Procedure Microfabrication of Three-Dimensional $\text{Co}_3\text{O}_4/\text{Pt}$ Nanonetwork for High-Performance Microsupercapacitors

Xinyu Ma,^a Shuxuan Feng,^a Liang He,^{*ab} Mengyu Yan,^a Xiaocong Tian,^a Yanxi Li,^c Chunjuan Tang,^{ad} Xufeng Hong,^a Liqiang Mai^{*ae}

a State Key Laboratory of Advanced Technology for Materials Synthesis and Processing, Wuhan University of Technology, Wuhan 430070, P. R. China

b Department of Materials Science and NanoEngineering, Rice University, 6100 Main Street, Houston, TX 77005, United States

c Department of Materials Science and Engineering, Virginia Tech, Blacksburg, Virginia 24061, USA

d Department of Mathematics and Physics, Luoyang Institute of Science and Technology, Luoyang 471023, P. R. China

e Department of Chemistry, University of California-Berkeley, Berkeley, California 94702, United States

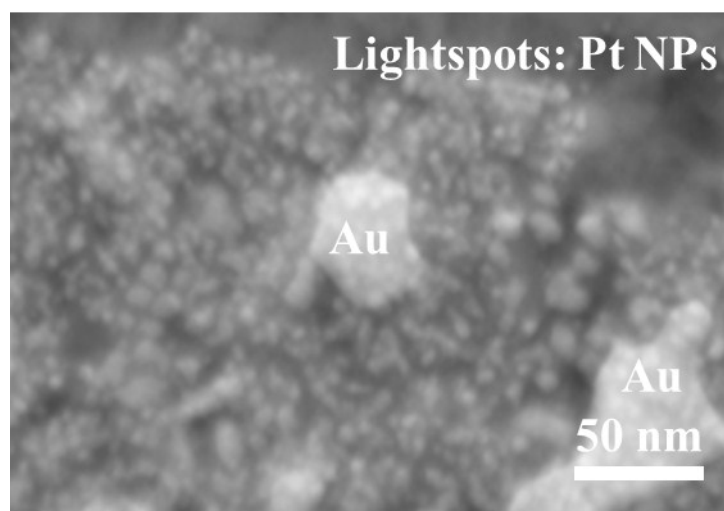


Figure S1 Dark-field TEM image of $\text{Co}_3\text{O}_4/\text{Pt}$ microelectrode.

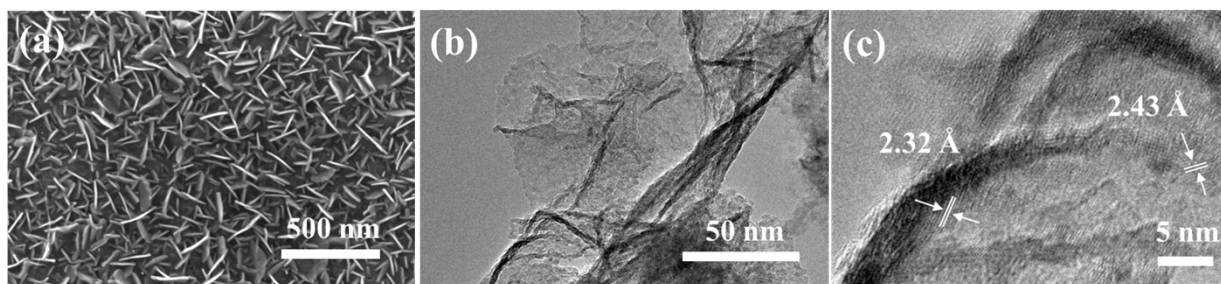


Figure S2 a) FESEM image of Co_3O_4 nanonetwork on the interdigital microelectrode. b-c) TEM and HRTEM images of Co_3O_4 nanonetwork.

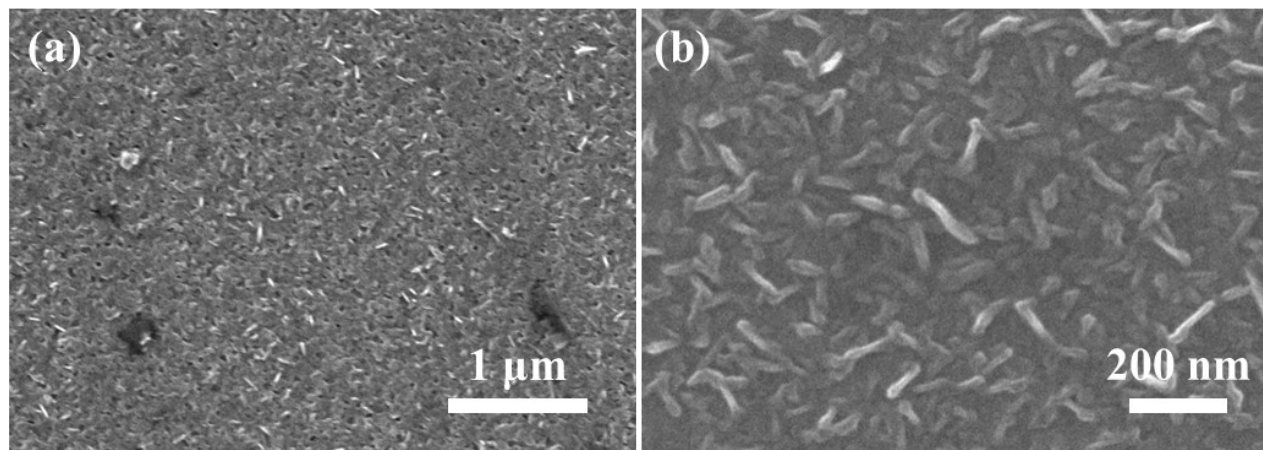


Figure S3 a-b) FESEM images of $\text{Co}_3\text{O}_4/\text{Pt}$ microelectrode after annealing at $450\text{ }^\circ\text{C}$ for 5 minutes.

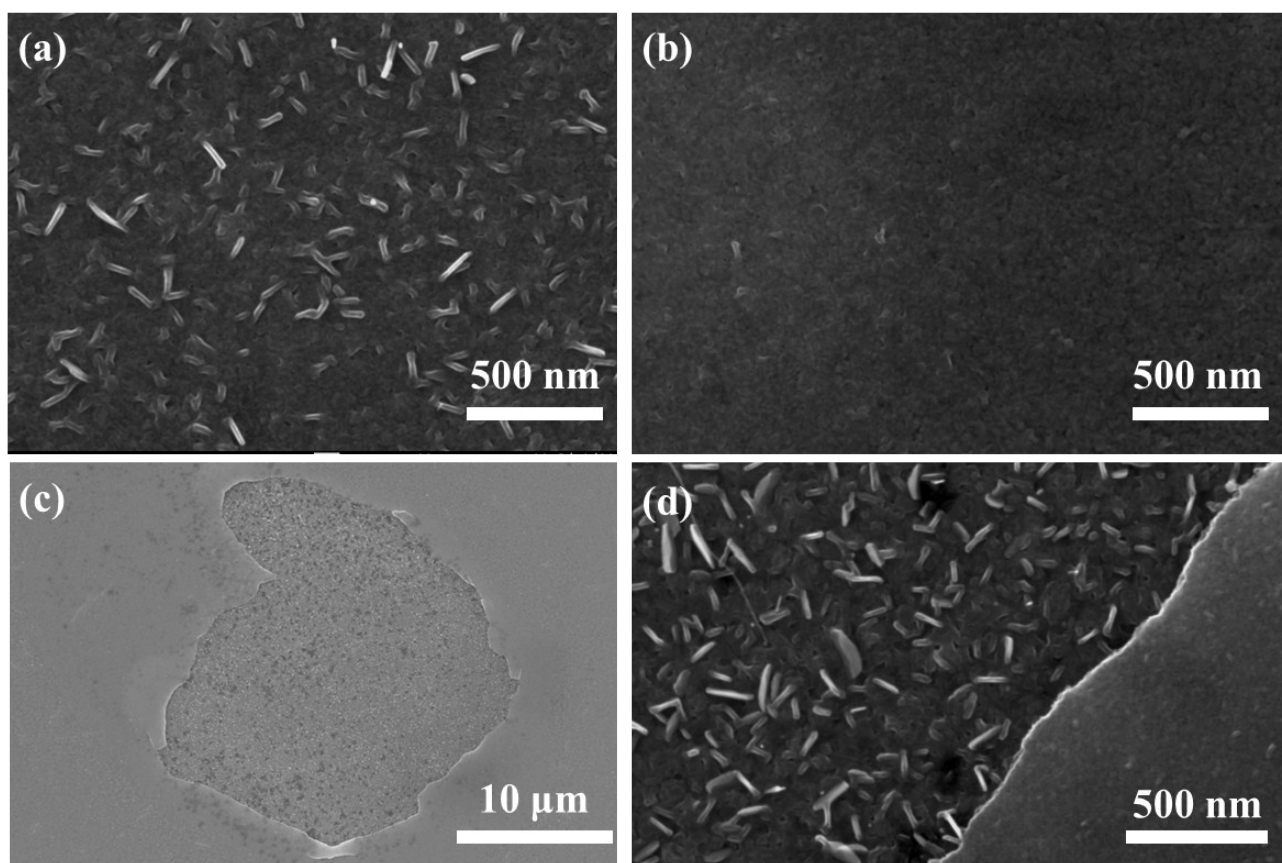


Figure S4 FESEM images of $\text{Co}_3\text{O}_4/\text{Pt}$ microelectrodes with different Pt NPs sputtering time of 160 s (a) and 240 s (b-d).

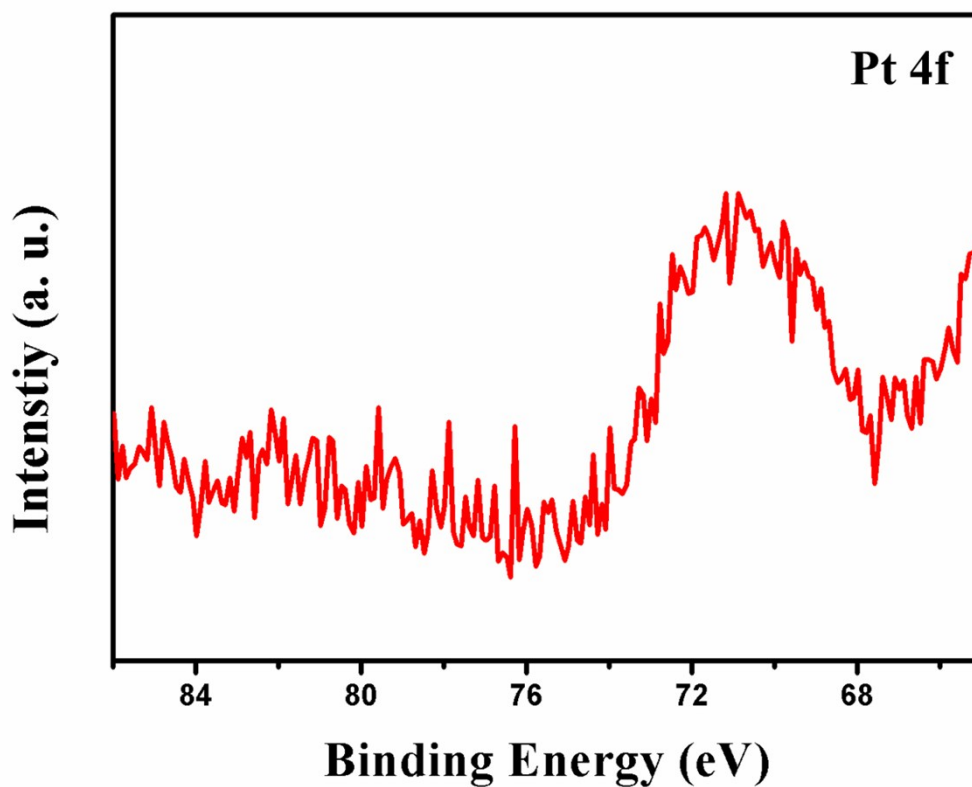


Figure S5 XPS spectrum of the Pt 4f binding energy region of $\text{Co}_3\text{O}_4/\text{Pt}$ microelectrode

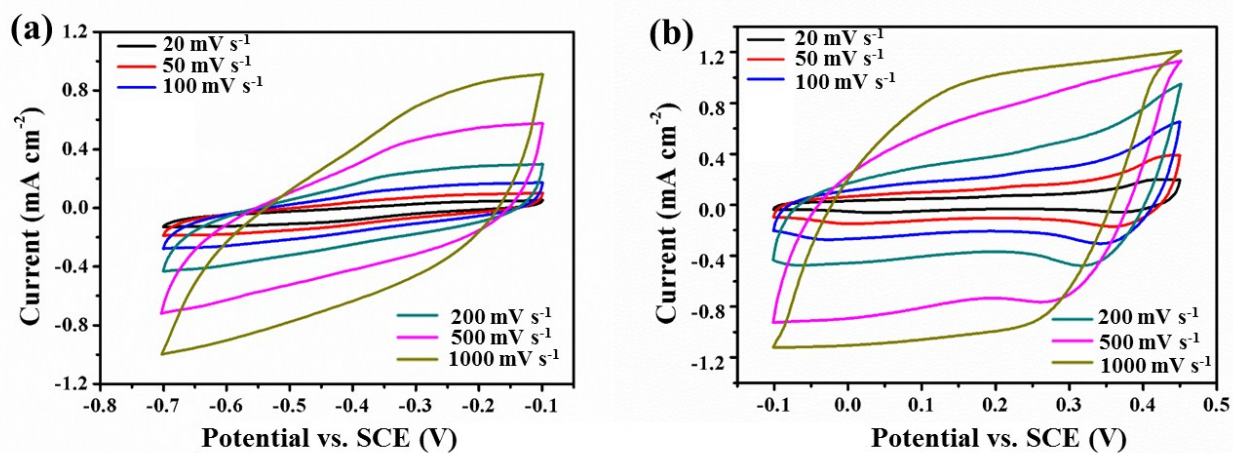


Figure S6 CV curves of $\text{Co}_3\text{O}_4/\text{Pt}$ MSC with potential window from a) -0.7 to -0.1 V vs. SCE and b) -0.1 to 0.45 V vs. SCE.

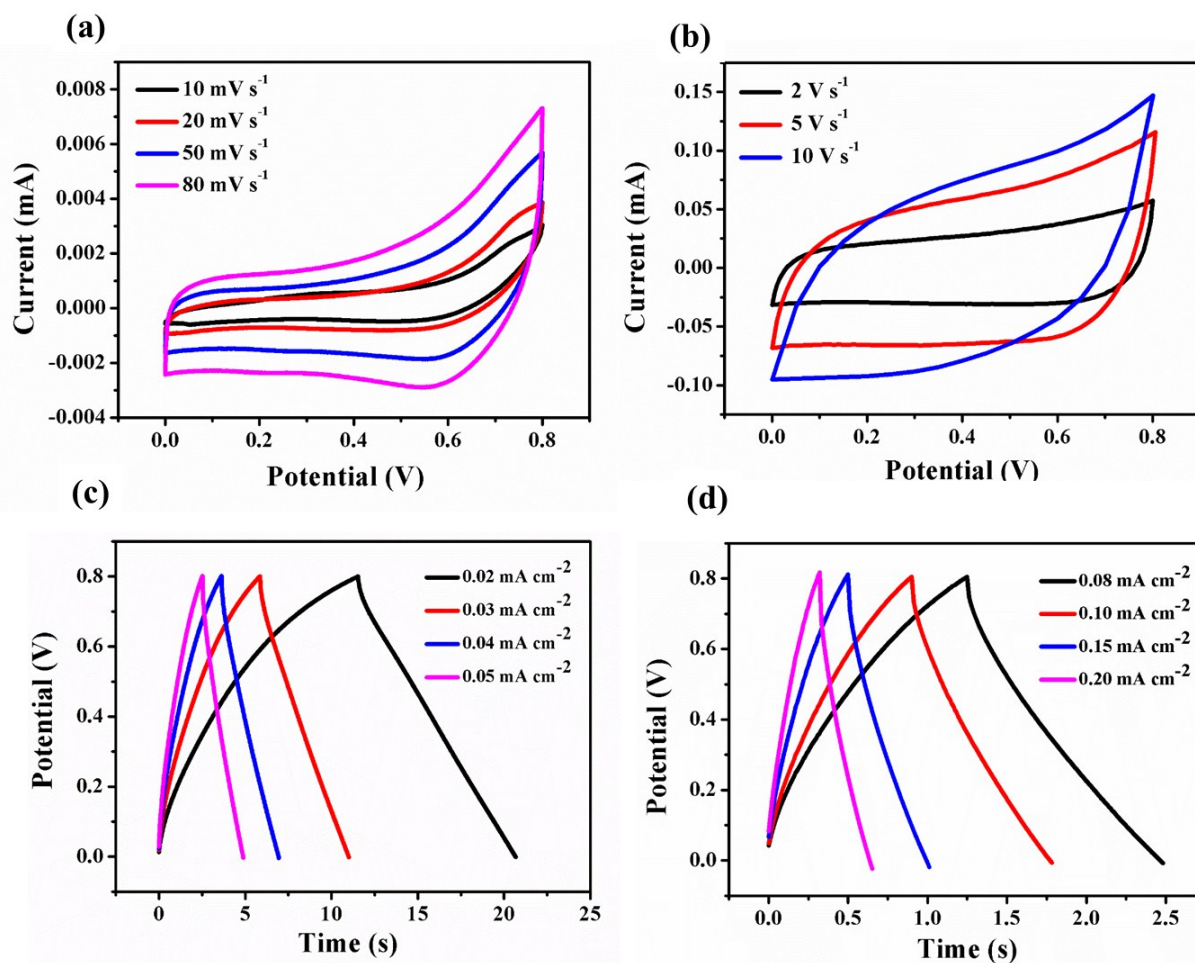


Figure S7 a-b) CV curves of Co_3O_4 MSC at different scan rates in 1 M KOH with potential window from 0 to 0.8 V. c-d) Galvanostatic charge/discharge curves of Co_3O_4 MSC at various current densities.

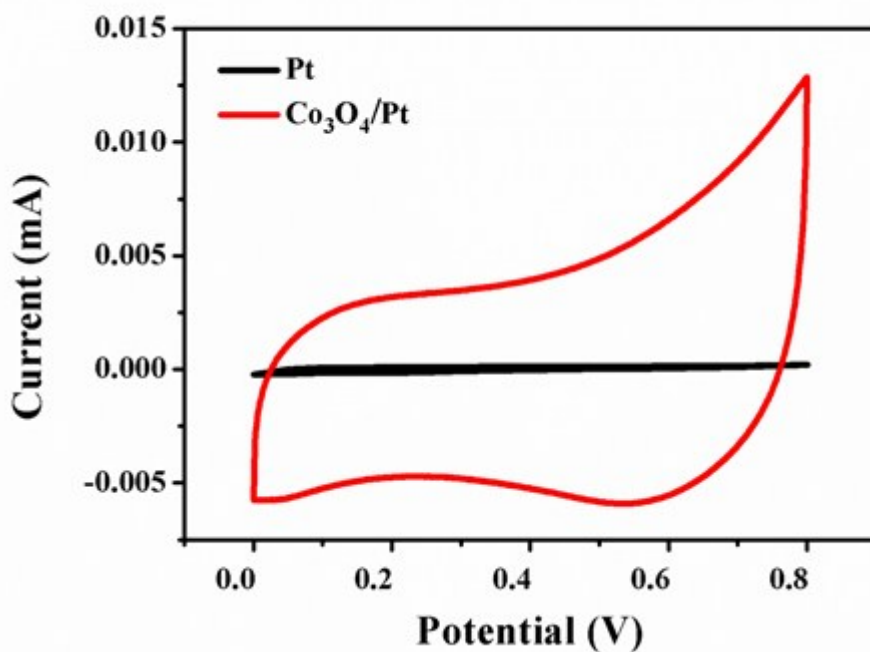


Figure S8 CV curves of Pt and Co_3O_4 MSCs.

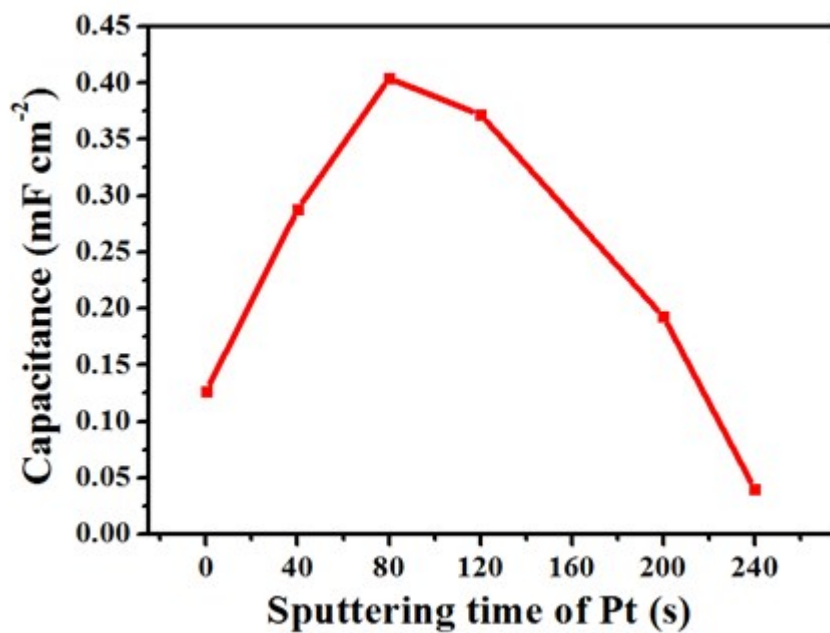


Figure S9 The areal capacitances of Co₃O₄/Pt MSCs with different sputtering time of Pt NPs.

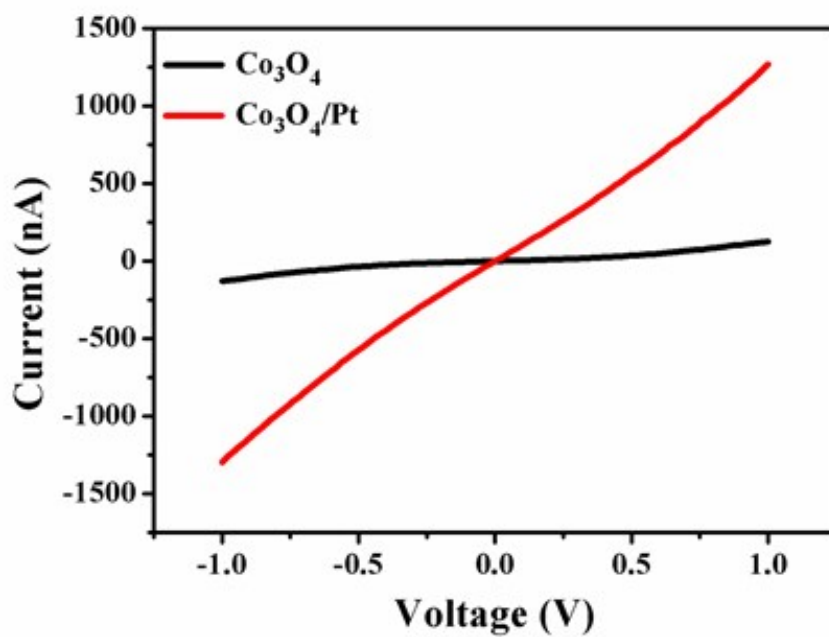


Figure S10 I-V curves of Co₃O₄ and Co₃O₄/Pt microelectrodes.

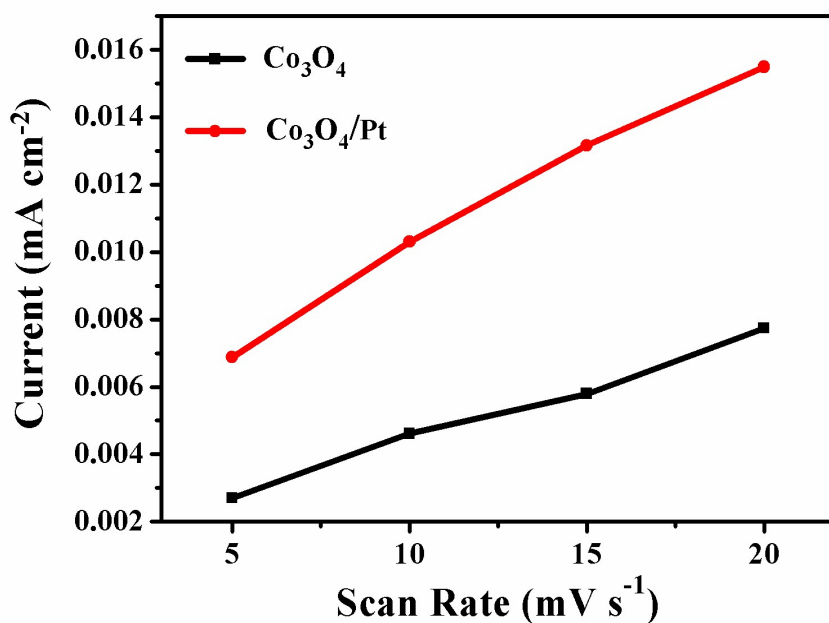


Figure S11 EDLC currents of Co₃O₄ and Co₃O₄/Pt MSCs

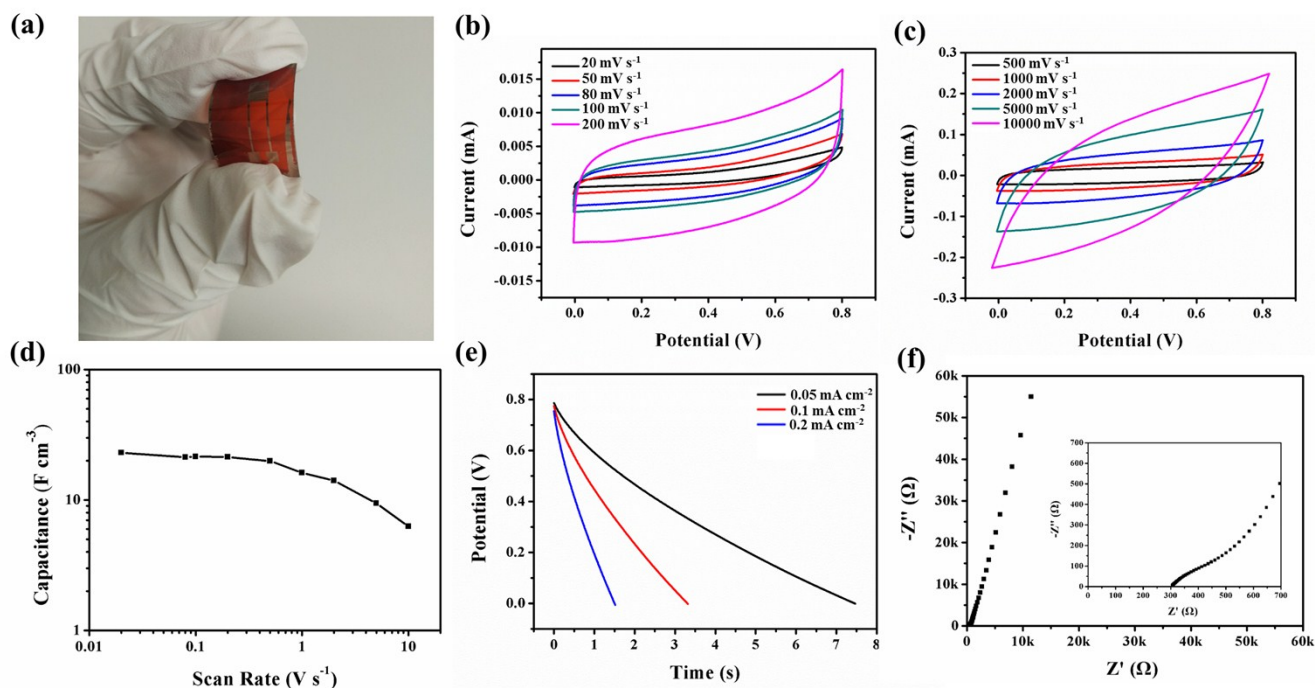


Figure S12 a) Digital image of a flexible Co₃O₄/Pt MSC. b-c) CV curves of flexible Co₃O₄/Pt MSC at different scan rates with potential window from 0 to 0.8 V. d) The volume capacitance of Co₃O₄/Pt MSC at different scan rates. e) Galvanostatic charge/discharge curves of Co₃O₄/Pt MSC at various current densities. f) Nyquist plots of Co₃O₄/Pt and Co₃O₄ MSCs. The inset shows the high-frequency region.

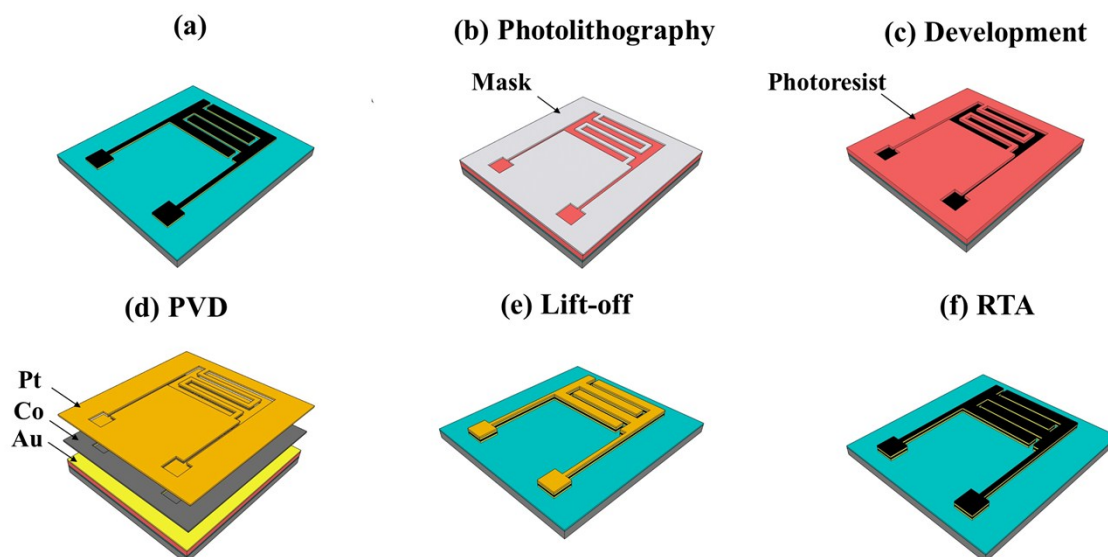


Figure S13 a-f) Schematic illustration of the microfabrication process of on-chip DMSC

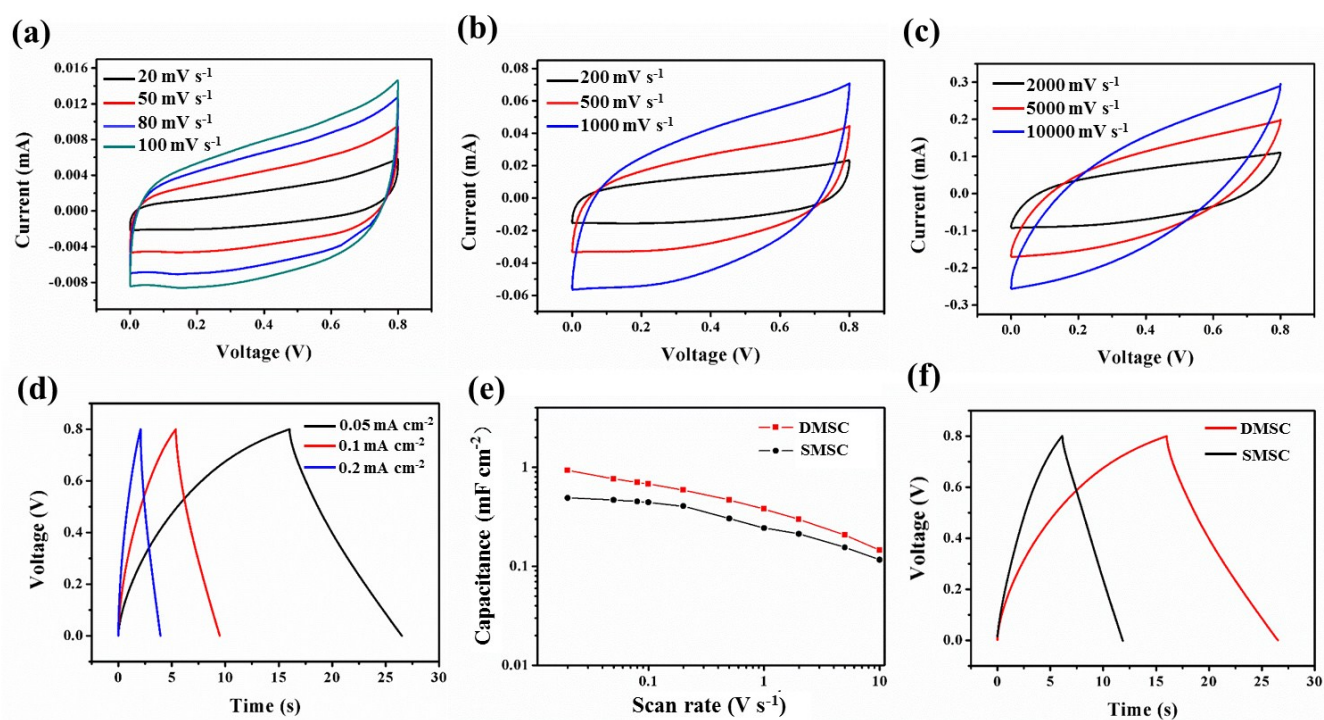


Figure S14 a-c) CV curves of DMSC at different scan rates with potential window from 0 to 0.8 V. d) Galvanostatic charge/discharge curves of DMSC at various current densities e) Evolution of the area capacitance of DMSC and SMSC at different scan rates. f) Galvanostatic charge/discharge curves of DMSC and SMSC at a current density of 0.05 mA cm^{-2} .